Mathematical Biosciences and Engineering

http://www.aimspress.com/journal/mbe

MBE, 20(2): 3793–3810.
DOI: 10.3934/mbe.2023178
Received: 12 October 2022
Revised: 28 November 2022
Accepted: 02 December 2022
Published: 12 December 2022

Research article

Practical discontinuous tracking control for a permanent magnet synchronous motor

Bin Liu[1], Dengxiu Yu[2,*], Xing Zeng[1], Dianbiao Dong[1], Xinyi He[3] and Xiaodi Li[3,4,*]

[1] School of Mechanical Engineering, Northwestern Polytechnical University, Xi'an 710072, China
[2] Unmanned System Research Institute, Northwestern Polytechnical University, Xi'an 710072, China
[3] School of Mathematics and Statistics, Shandong Normal University, Ji'nan 250014, China
[4] Department of Automation, Tsinghua University, Beijing 100084, China

* **Correspondence:** Email: yudengxiu@nwpu.edu.cn, lxd@sdnu.edu.cn.

Abstract: In this paper, the practical discontinuous control algorithm is used in the tracking controller design for a permanent magnet synchronous motor (PMSM). Although the theory of discontinuous control has been studied intensely, it is seldom applied to the actual systems, which encourages us to spread the discontinuous control algorithm to motor control. Due to the constraints of physical conditions, the input of the system is limited. Hence, we design the practical discontinuous control algorithm for PMSM with input saturation. To achieve the tracking control of PMSM, we define the error variables of the tracking control, and the sliding mode control method is introduced to complete the design of the discontinuous controller. Based on the Lyapunov stability theory, the error variables are guaranteed to converge to zero asymptotically, and the tracking control of the system is realized. Finally, the validity of the proposed control method is verified by a simulation example and the experimental platform.

Keywords: discontinuous control; motor; sliding mode control; input saturation; tracking control

1. Introduction

In recent years, the control problem of time-varying systems has been widely considered [1–4], and most control protocols of time-varying systems are based on continuous control methods [5–9], which require continuous control input. However, discontinuous control [10, 11] is more effective in some specific cases, and it has attracted more and more attention from researchers. Although the theoretical research on discontinuous control strategy is abundant, few researchers have applied it to practical systems, which motivates us to use this method in actual scenarios. In addition, the input of the actual system is limited, and the control input based on the traditional approach is likely to exceed the limit

and affect the control performance of the controller. Thus, input saturation can-not be ignored in the process of controller design. According to the above analysis, we study the practical discontinuous control of PMSM and complete the design of an intermittent controller by the sliding mode control method.

Discontinuous control strategy includes impulsive control [12, 13], intermittent control, and sampling control. According to the division of the control cycle, intermittent control is divided into periodic and non-periodic intermittent control. In [14, 15], a novel control strategy consisting of an event-triggering mechanism and impulsive control showed its effectiveness in stabilizing nonlinear systems and can effectively reduce the cost of signal transmission. To solve the leader-follower synchronization problem in complex networks [16, 17], a batch control scheme based on being dual event-driven was proposed. In [18], the observer-based state feedback non-periodic intermittent control for uncertain systems with structural uncertainty was studied. A class of finite-time synchronous control of reaction-diffusion nervous systems coupled with small regions with interaction diagrams on spatial boundaries was researched in [19]. In [20], the intermittent control strategy for synchronous analysis of time-varying complex dynamic networks was studied, and some numerical simulations verified the validity of the results. Although discontinuous control has received much attention from researchers, most of the above research remains at the stage of theoretical research. To improve the practical ability of the algorithm, we carry out the research of applying the discontinuous control algorithm to motor control.

For a real system, the limit of input saturation can not be ignored. Input saturation [21, 22] often seriously affects the performance of the system and even leads to system instability. In [23], the global stabilization problem of discrete-time linear systems with input saturation and delay was studied, and three examples demonstrated the effectiveness of the proposed method. In [24], the researchers studied the consistency of a class of linear multi-agent systems with input saturation under a self-triggering mechanism. The adaptive control strategy of the flexible manipulator with a double pendulum structure was analyzed, and the effectiveness of the saturation controller in tracking control was verified in [25]. The tracking control problem for nonlinear stochastic systems with time-varying state constraints and input saturation was studied in [26]. In [27], adaptive fuzzy tracking control for high-order nonlinear time-delay systems with full state constraints and input saturation was studied. Considering that the input is bounded in the real system, the input saturation auxiliary system is used to compensate for the influence of input saturation on the control performance, which makes our algorithm more valuable in the application.

Currently, many control methods are applied to controller design, such as the backstepping method [28, 29], model predictive control and sliding mode control [30, 31]. As one of the common control methods, sliding mode control has a wide range of application scenarios [32, 33]. In [34], the sliding mode control of uncertain linear systems with impulsive effects was studied, and the stability of the system was analyzed by piecewise discontinuous Lyapunov function. A robust fault-tolerant compensation control method based on the integral sliding mode method was proposed for uncertain linear systems on networks [35]. In [36], the researchers considered unknown asymmetric input saturation and control singularity and designed a fuzzy terminal sliding mode controller based on the disturbance observer. In [37], a new sliding mode switching approximation law was proposed to improve sliding mode control performance for a class of high-order self-organizing systems. The problem of event-triggered fuzzy sliding mode control for networked control systems with semi-Markov process adjust-

ment was studied in [38]. To design a practical discontinuous controller with input saturation, sliding mode control is used in the design of the control algorithm to achieve the desired control objective.

Through the above analysis, we consider the practical discontinuous tracking control problem of PMSM under input saturation and use the sliding mode control method to complete the design of the controller. The main contributions of this paper are described as follows:

1) To improve the applicability of the discontinuous control method, we apply the discontinuous control method to the tracking control of PMSM and carry out the experimental verification. However, most of the previous discontinuous control is at the level of theoretical research and rarely applied to the actual system.

2) Due to physical constraints, we consider the input saturation in the actual scenario. By introducing the input saturation auxiliary system, we reduce the influence of input saturation on the system and calculate the theoretical control input of the system.

3) To realize the discontinuous control of PMSM, sliding mode control is introduced into the design of the discontinuous controller, which ensures the stability and robustness of the system under the input of discontinuous control.

The remaining part of the paper is described as follows. Some essential knowledge and a necessary lemma are introduced in Section 2. We use the sliding mode control method to complete the design of the discontinuous controller and provide the stability analysis in Section 3. We resort to the simulation results to verify the availability of the controller design in Section 4. In Section 5, the experimental platform demonstrates the effectiveness of the practical discontinuous control algorithm. In Section 6, we summarize the whole paper.

2. Preliminaries and problem formulation

This section introduces the definitions of intermittent control, systems model, and input saturation, which will be used in the rest of the work.

2.1. Discontinuous control

Intermittent control is one of the strategies of discontinuous control. The division of the control cycle can be divided into periodic intermittent control and aperiodic intermittent control. In this paper, we adopt the periodic intermittent control strategy. The main design idea is to divide the whole control cycle into equal intervals T of the control cycle. Each control period is divided into the controlled period and the uncontrolled period. The two continuous control periods, n and $n+1$, are described in Figure 1, and $n = 0, 1, 2, \cdots$.

When $t \in [nT, nT + \eta]$, at nT moment, the system receives instructions from the controller, and at $nT + \eta$ moment, the control instruction ends. Thus, $[nT, nT + \eta]$ is the controlled period of the system. During the period of $[nT + \eta, (n+1)T]$, the system does not receive any instructions from the controller. Thus, $[nT + \eta, (n + 1)T]$ is the uncontrolled period of the system. In addition, in periodic intermittent control, the control amplitude $\eta = nT + \eta - nT > 0$ is a constant value.

Lemma 1. *(Young's inequality) For arbitrary positive real numbers x and y, the following inequality holds.*

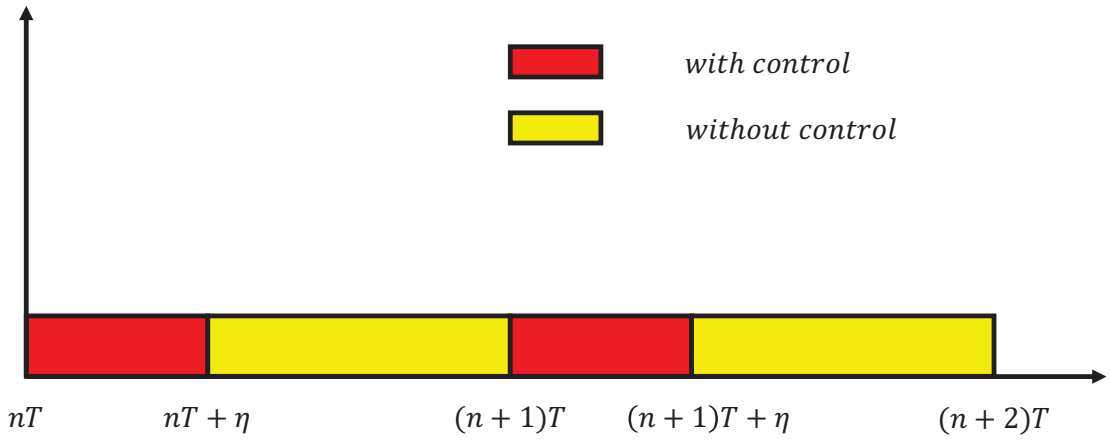

Figure 1. Graphical explanation of intermittent control strategy.

$$xy \le \frac{x^a}{a} + \frac{y^b}{b} \tag{2.1}$$

where $a > 0$ and $b > 0$, with $(a-1)(b-1) = 1$. If and only if $x^a = y^b$, the equality sign holds.

Definition 1. *Considering the impact of input saturation, the actual control input* $u\left(i_q\right)$ *is the nonlinear function of ideal control input* i_q*. The* $u\left(i_q\right)$ *is defined as follows*

$$u\left(i_q\right) = sat\left(i_q\right) = \begin{cases} i_q & |i_q| \le i_M \\ i_M \cdot sgn\left(i_q\right) & |i_q| > i_M \end{cases} \tag{2.2}$$

where i_M *is the boundary of control input saturation.*

2.2. The dynamic model of the PMSM and system descriptions

The dynamic model of a 3-phase PMSM can be described as [39]

$$\begin{cases} J\frac{d\omega}{dt} = T_e - T_l - f\omega \\ T_e = \frac{3}{2}pi_q\left[i_d\left(L_d - L_q\right) + \Phi\right] \end{cases} \tag{2.3}$$

where J is the moment of inertia, ω is the angular velocity , and T_e and T_l are the electromagnetic torque and load torque, respectively. f is the damping coefficient. p represents the number of pairs of the permanent magnet rotor poles. L_d and L_q are the inductance of the d-q axis, and i_d and i_q represent the d-q axis parts of stator current. Φ is the permanent magnet flux linkage.

Normally, the space vector pulse-width modulation control method of $i_d = 0$ is used for the 3-phase PMSM with the surface-mounted permanent magnet rotor. Hence, we can the following formula [40].

$$L_d = L_q = L_s \tag{2.4}$$

where L_s is the inductance of the stator.

According to Definition 1, (2.3) and (2.4), the dynamic model under input saturation can be described as the following:

$$\begin{cases} \dot{\theta}_1 = \omega_1 \\ \dot{\omega}_1 = \dfrac{3}{2}\dfrac{p\Phi}{J}u\left(i_q\right) - \dfrac{T_l}{J} - \dfrac{f}{J}\omega_1 \end{cases} \tag{2.5}$$

where θ_1 and ω_1 are angle and angular velocity, respectively.

Let $g = \frac{3}{2}\frac{p\Phi}{J}$, $d = -T_l/J$, $c = -f/J$, and (2.5) can be redescribed as

$$\begin{cases} \dot{\theta}_1 = \omega_1 \\ \dot{\omega}_1 = gu\left(i_q\right) + d + c\omega_1 \\ y_1 = \theta_1 \end{cases} \tag{2.6}$$

where i_q and y_1 are the ideal control input and output, respectively.

The dynamics of the reference signal are described as

$$\begin{cases} \dot{\theta}_2 = \omega_2 \\ \dot{\omega}_2 = d + c\omega_2 \\ y_2 = \theta_2 \end{cases} \tag{2.7}$$

where θ_2 and ω_2 are angle and angular velocity of the reference signal.

Control objective: In this paper, the control objective is to design the discontinuous controller with the sliding mode control method under the constraint of input saturation, such that the error variables ε_1 and ε_2 converge to zero asymptotically.

3. Discontinuous controller design and stability analysis

3.1. Discontinuous controller design

In this section, we design the discontinuous controller through sliding mode control to realize the tracking control to reference signal.

The structure diagram of the practical discontinuous controller is shown in Figure 2. The controller is mainly composed of the discontinuous controller, input saturation auxiliary system, input saturation actuator and PMSM. The dynamic control model of PMSM can be expressed by Eq (2.6), and the constraint effect of the input saturation actuator on the control input signal can be expressed by Eq (2.2). The design of other parts will be given in detail below.

For any $n \in \mathbb{Z}_+ \cup \{0\}, t \in (nT, (n+1)T)$, the error variables are described as follows :

$$\begin{cases} \varepsilon_1 = \theta_1 - \theta_2 - \int_0^t \xi dt + \int_0^{nT} \xi dt, \\ \varepsilon_2 = \omega_1 - \omega_2 - \xi, \end{cases} \tag{3.1}$$

where ε_1 and ε_2 are error variables. ξ is the input saturation auxiliary system, which will be designed in subsequent processes.

We define

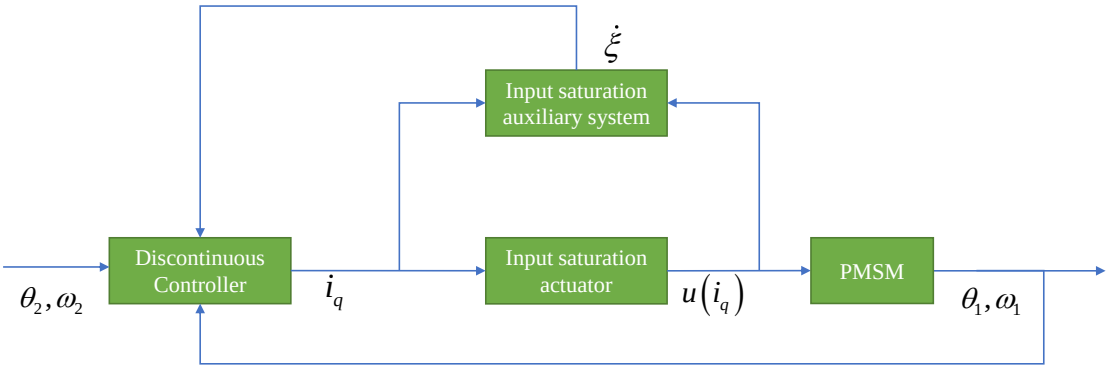

Figure 2. Block diagram of discontinuous controller.

$$\theta = \theta_1 - \theta_2, \tag{3.2}$$

$$\omega = \omega_1 - \omega_2, \tag{3.3}$$

$$\bar{\varepsilon} = \varepsilon_2 + k\varepsilon_1. \tag{3.4}$$

The time derivative of (3.1) is written as

$$\begin{cases} \dot{\varepsilon}_1 = \omega_1 - \omega_2 - \xi = \varepsilon_2, \\ \dot{\varepsilon}_2 = \dot{\omega}_1 - \dot{\omega}_2 - \dot{\xi} = \dot{\omega} - \dot{\xi}. \end{cases} \tag{3.5}$$

Case 1: For any $n \in \mathbb{Z}_+ \cup \{0\}, t \in [nT, nT + \eta)$, we construct the following Lyapunov function

$$V = \frac{1}{2}\left(\varepsilon_1^2 + \bar{\varepsilon}^2\right) \tag{3.6}$$

The time derivative of (3.6) is written as

$$\begin{aligned} \dot{V} &= \varepsilon_1\dot{\varepsilon}_1 + \bar{\varepsilon}\dot{\bar{\varepsilon}} \\ &= \varepsilon_1\varepsilon_2 + \bar{\varepsilon}\left(\dot{\varepsilon}_2 + k\dot{\varepsilon}_1\right). \end{aligned} \tag{3.7}$$

Substituting (3.5) into (3.7), we have

$$\begin{aligned} \dot{V} &= \varepsilon_1\left(\bar{\varepsilon} - k\varepsilon_1\right) + \bar{\varepsilon}\left(\dot{\omega} - \dot{\xi} + k\left(\omega_1 - \omega_2 - \xi\right)\right) \\ &= -k\varepsilon_1^2 + \bar{\varepsilon}\left(\dot{\omega} - \dot{\xi} + k(\omega - \xi) + \varepsilon_1\right) \end{aligned} \tag{3.8}$$

The input saturation auxiliary system ξ and ideal control input i_q are designed as follows:

$$\dot{\xi} = c\xi + gu\left(i_q\right) - gi_q, \ \xi(nT) = 0 \tag{3.9}$$

$$i_q = -\frac{1}{g}\left[\left((2k + c)\varepsilon_2 + \left(k^2 + 1\right)\varepsilon_1\right)\right] \tag{3.10}$$

Substituting (3.9) into (3.8), we can obtain

$$\begin{aligned}\dot{V} &= -k\varepsilon_1^2 + \bar{\varepsilon}\left(\dot{\omega} - \dot{\xi} + k(\omega - \xi) + \varepsilon_1\right)\\ &= -k\varepsilon_1^2 + \bar{\varepsilon}\left(\dot{\omega} - c\xi - gu\left(i_q\right) + gi_q + k(\omega - \xi) + \varepsilon_1\right)\\ &= -k\varepsilon_1^2 + \bar{\varepsilon}\left((k+c)\cdot(\omega - \xi) + gi_q + \varepsilon_1\right)\\ &= -k\varepsilon_1^2 + \bar{\varepsilon}\left((k+c)\cdot\varepsilon_2 + gi_q + \varepsilon_1\right)\end{aligned} \tag{3.11}$$

Substituting (3.10) into (3.11), we have

$$\begin{aligned}\dot{V} &= -k\left(\varepsilon_1^2 + \bar{\varepsilon}^2\right)\\ &= -2kV.\end{aligned} \tag{3.12}$$

Case 2: For $t \in [nT + \eta, (n+1)T)$ and there holds that

$$\begin{aligned}\dot{V} &= \varepsilon_1\dot{\varepsilon}_1 + \bar{\varepsilon}\dot{\varepsilon}\\ &= \varepsilon_1\varepsilon_2 + \bar{\varepsilon}\left(\dot{\varepsilon}_2 + k\dot{\varepsilon}_1\right)\\ &= \varepsilon_1\left(\bar{\varepsilon} - k\varepsilon_1\right) + \bar{\varepsilon}\left(\dot{\omega} - \dot{\xi} + k\left(\omega_1 - \omega_2 - \xi\right)\right)\\ &= -k\varepsilon_1^2 + \bar{\varepsilon}\left(\dot{\omega} - \dot{\xi} + k(\omega - \xi) + \varepsilon_1\right)\end{aligned} \tag{3.13}$$

The input saturation auxiliary system ξ and control input u are designed as follows

$$\dot{\xi} = c\xi + gu\left(i_q\right) - gi_q \tag{3.14}$$

$$i_q = 0. \tag{3.15}$$

Substituting (3.14) and (3.15) into (3.13), we can obtain

$$\begin{aligned}\dot{V} &= -k\varepsilon_1^2 + \bar{\varepsilon}\left(\dot{\omega} - c\xi - gu\left(i_q\right) + gi_q + k(\omega - \xi) + \varepsilon_1\right)\\ &= -k\varepsilon_1^2 + \bar{\varepsilon}\left((k+c)\cdot(\omega - \xi) + \varepsilon_1\right)\\ &= -k\varepsilon_1^2 + \bar{\varepsilon}\left((k+c)\cdot\varepsilon_2 + \varepsilon_1\right).\end{aligned} \tag{3.16}$$

Substituting (3.4) into (3.16), we can obtain

$$\begin{aligned}\dot{V} &= -k\varepsilon_1^2 + (k+c)\bar{\varepsilon}\varepsilon_2 + \bar{\varepsilon}\varepsilon_1\\ &= -k\varepsilon_1^2 + (k+c)\bar{\varepsilon}^2 - k(k+c)\bar{\varepsilon}\varepsilon_1 + \bar{\varepsilon}\varepsilon_1\\ &= [1 - k(k+c)]\bar{\varepsilon}\varepsilon_1 - k\varepsilon_1^2 + (k+c)\bar{\varepsilon}^2.\end{aligned} \tag{3.17}$$

According to Lemma 1, we have

$$\begin{aligned}[1 - k(k+c)]\bar{\varepsilon}\varepsilon_1 &\le (|1 - k(k+c)|)|\bar{\varepsilon}\varepsilon_1|\\ &\le \frac{1}{2}(|1 - (k+c)k|)(\varepsilon_1^2 + \bar{\varepsilon}^2).\end{aligned} \tag{3.18}$$

Substituting (3.18) into (3.17), we can obtain

$$\begin{aligned}\dot{V} &\leq \frac{1}{2}(|1-(k+c)k|)\left(\varepsilon_1^2+\bar{\varepsilon}^2\right)-k\varepsilon_1^2+(k+c)\bar{\varepsilon}^2\\ &\leq \frac{1}{2}[(|1-(k+c)k|)+(k+c)]\left(\varepsilon_1^2+\bar{\varepsilon}^2\right)\\ &\leq k_0 V\end{aligned} \tag{3.19}$$

where $k_0 = |1-(k+c)k| + (k+c)$, $2k + c > 0$.

3.2. Stability analysis

Case 1: For any $n \in \mathbb{Z}_+ \cup \{0\}, t \in [nT, nT+\eta)$, we have

$$\dot{V} = -2kV. \tag{3.20}$$

Then, we have

$$V(nT+\eta) = e^{-2k\eta}V(nT). \tag{3.21}$$

Proof : Multiplying both sides by e^{2kt}, (3.20) becomes

$$\frac{d}{dt}(V(t)e^{2kt}) = 0. \tag{3.22}$$

Integrating it over $[nT, nT+\eta]$, we have

$$V(nT+\eta) = e^{-2k\eta}V(nT). \tag{3.23}$$

Case 2: For any $n \in \mathbb{Z}_+ \cup \{0\}, t \in [nT+\eta, (n+1)T)$, we have

$$\dot{V} \leq k_0 V. \tag{3.24}$$

Similarly, we have

$$V((n+1)T) \leq e^{k_0(T-\eta)}V(nT+\eta). \tag{3.25}$$

According to (3.23) and (3.25)

$$\begin{aligned}V((n+1)T) &\leq e^{k_0(T-\eta)}V(nT+\eta)\\ &\leq e^{k_0(T-\eta)-2k\eta}V(nT).\end{aligned} \tag{3.26}$$

Therefore, when the inequality

$$\frac{\eta}{T} > \frac{k_0}{k_0+2k} \tag{3.27}$$

holds the function $V(t)$ is a monotonically decreasing continuous function.

$$\lim_{t\to\infty} V(t) = 0 \tag{3.28}$$

According to (3.6), we have

$$\lim_{t\to\infty} V(t) = \frac{1}{2}\left(\varepsilon_1^2 + \bar{\varepsilon}^2\right) = 0. \tag{3.29}$$

This indicates that

$$\begin{cases} \varepsilon_1 = \theta_1 - \theta_2 - \int_0^t \xi dt + \int_0^{nT} \xi dt = 0, \\ \varepsilon_2 = \omega_1 - \omega_2 - \xi = 0. \end{cases} \tag{3.30}$$

Thus, when $t \to \infty$, we have

$$i_q = -\frac{1}{g}\left[\left((2k + c)\varepsilon_2 + \left(k^2 + 1\right)\varepsilon_1\right)\right] = 0. \tag{3.31}$$

Then, at the moment $0 < t_1 < \infty$, $t_1 \in [(n-1)T, nT)$, $i_q \le i_M$, $u\left(i_q\right) = i_q$, the following equality holds:

$$\begin{aligned} &\dot{\xi} = c\xi + gu\left(i_q\right) - i_q = c\xi,\ \xi(nT) = 0, && t_2 \in [nT, nT + \eta), \\ &\dot{\xi} = c\xi, && t_2 \in [nT + \eta, (n+1)T). \end{aligned} \tag{3.32}$$

Further, we can obtain

$$\xi(t_2) = e^{c(t_2 - nT)}\xi(nT) = 0 \tag{3.33}$$

where $t_2 > nT$.

Thus, when $t \to \infty$, we have

$$\begin{cases} \varepsilon_1 = \theta_1 - \theta_2 = 0, \\ \varepsilon_2 = \omega_1 - \omega_2 = 0. \end{cases} \tag{3.34}$$

According to the above analysis, when $t \to \infty$, the tracking control target is accomplished. Simultaneously, there are $\theta_1 = \theta_2$ and $\omega_1 = \omega_2$.

4. Simulation example

The simulation design parameters are designed as $c = -2.1, d = 0, k = 2, g = 200, \eta/T = 0.5 > 0.22$ and $i_M = 5$. The initial values of the system are selected as $\theta_1(0) = 0, \omega_1(0) = 0, \theta_2(0) = 50, \omega_2(0) = 800$ and $\xi(0) = 0$.

Figures 3–10 show the simulation results of two kinds of control methods. Figure 3 displays the trajectories of θ_1 and θ_2. Figure 4 displays the trajectories of ω_1 and ω_2. The trajectories of error variables ε_1 and ε_2 are shown in Figures 5 and 6, respectively. From Figures 3–6, the simulation results indicate the proposed discontinuous control algorithm is valid. The trajectories of the control input i_q are exhibited in Figure 7. Figure 8 exhibits the trajectories of saturated input $u(i_q)$. The trajectories of input saturation auxiliary system ξ are shown in Figure 9. The trajectories of signals $\int_0^t \xi dt - \int_0^{nT} \xi dt$ are exhibited in Figure 10. The comparison results show that the discontinuous controller designed in this paper can achieve similar control effects to the continuous controller.

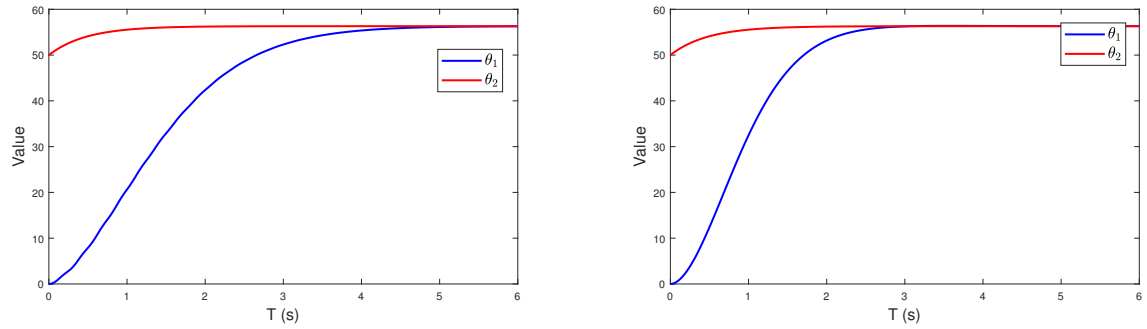

(a) (b)

Figure 3. The trajectories of system state of θ_1 and θ_2. (a) Discontinuous control. (b) Continuous control.

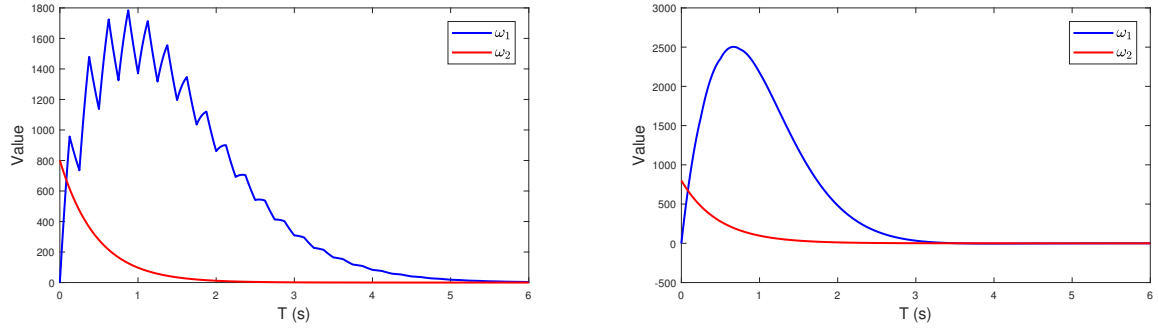

(a) (b)

Figure 4. The trajectories of system state of ω_1 and ω_2. (a) Discontinuous control. (b) Continuous control.

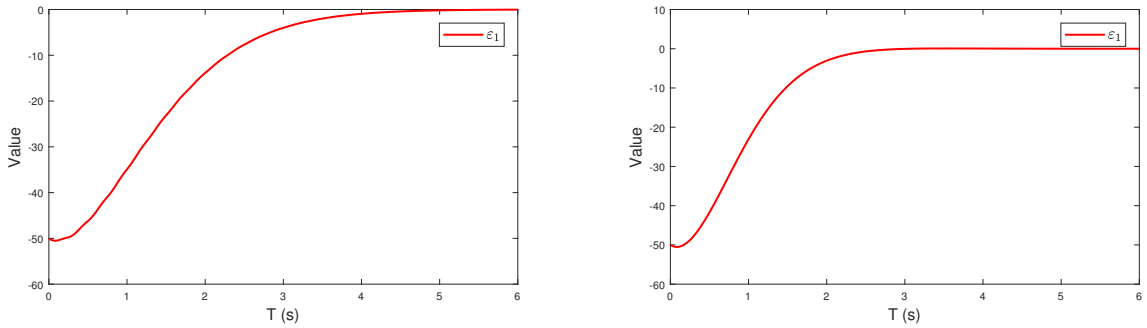

(a) (b)

Figure 5. The trajectories of error variables ε_1. (a) Discontinuous control. (b) Continuous control.

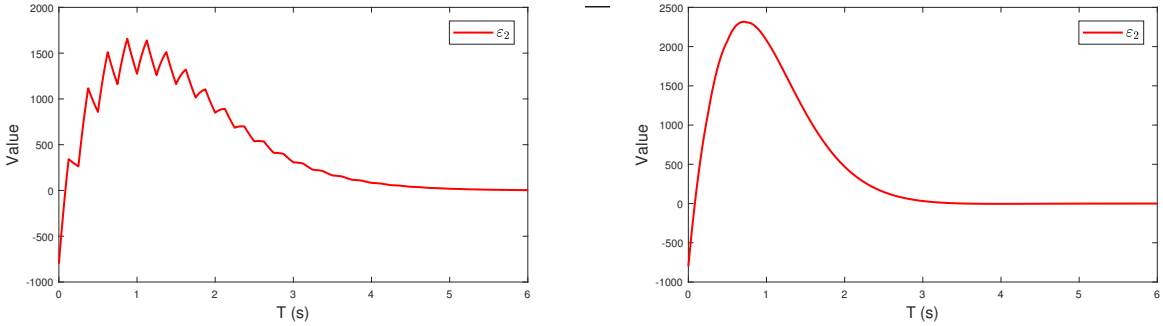

(a) (b)

Figure 6. The trajectories of error variables of ε_2. (a) Discontinuous control. (b) Continuous control.

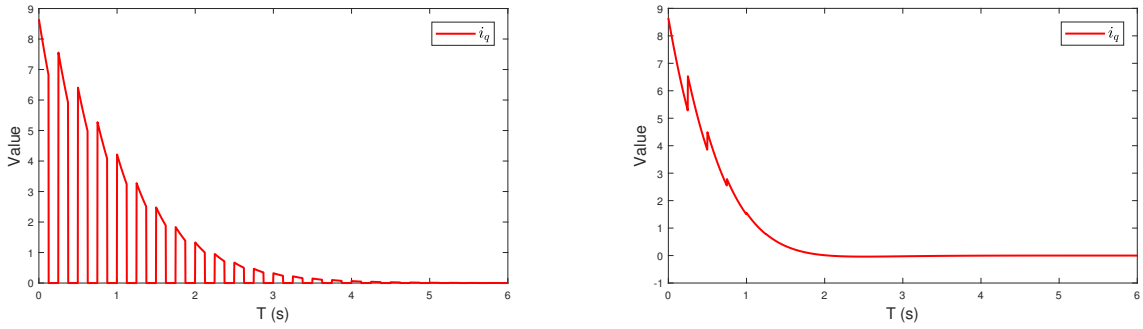

(a) (b)

Figure 7. The trajectories of input i_q. (a) Discontinuous control. (b) Continuous control.

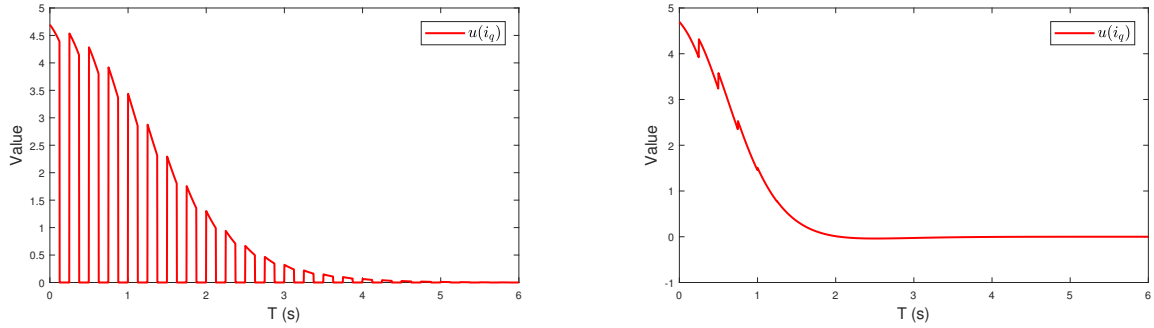

(a) (b)

Figure 8. The trajectories of saturated input $u(i_q)$. (a) Discontinuous control. (b) Continuous control.

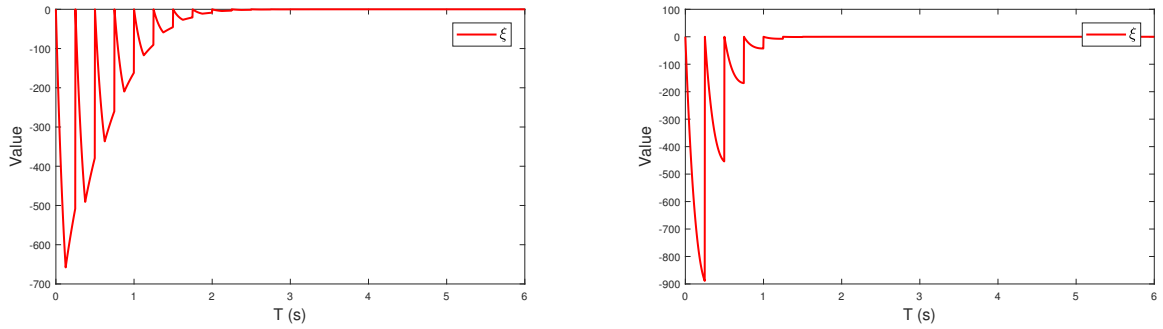

(a) (b)

Figure 9. The trajectories of input saturation auxiliary system ξ. (a) Discontinuous control. (b) Continuous control.

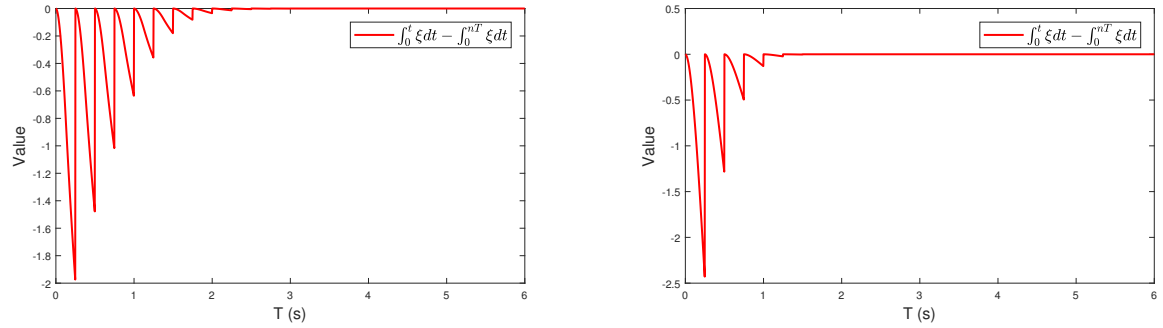

(a) (b)

Figure 10. The trajectories of signals $\int_0^t \xi dt - \int_0^{nT} \xi dt$. (a) Discontinuous control. (b) Continuous control.

5. Experimental results

The bicycle robot is a high-performance robot that integrates bicycles and intelligent control. It has both the convenience and flexibility of bicycles and the high intelligence of integrated control systems. Bicycle robots can replace human work on specific occasions, and they have broad application prospects in rescue and disaster relief, industrial production and resource exploration. The intermittent control algorithm designed in this paper has great application value in the balance control problem of the balance bicycle. Based on this, we carry out the experimental test of the intermittent control algorithm for a single balance control motor of the balance bike, which is shown in Figure 11. It can be seen that the system consists of a DC power source, a controller and a motor. The communication network is based on the controller area network (CAN). Figure 12 displays the trajectories of θ_1 and θ_2. Figure 13 shows the trajectories of ω_1 and ω_2. Figure 14 exhibits the trajectories of saturated input $u(i_q)$.

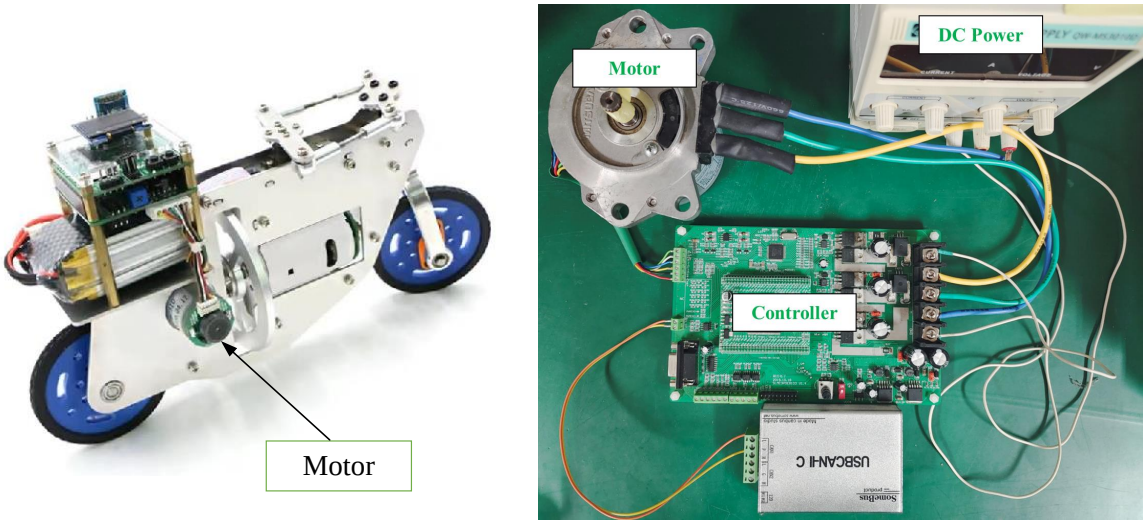

(a) (b)

Figure 11. The photograph of experimental platform. (a)balance bike. (b)Actual control of the motor unit.

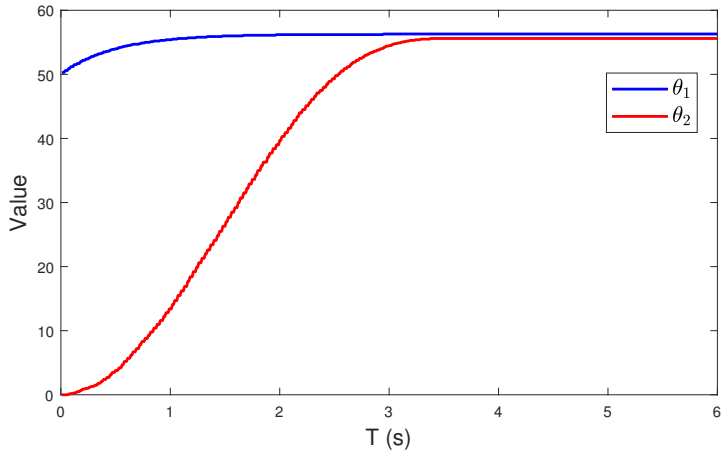

Figure 12. The trajectories of system state of θ_1 and θ_2.

6. Conclusions

In this paper, we complete the PMSM tracking controller design by the practical discontinuous control algorithm. An input saturation auxiliary system is introduced to ensure the practicality of the controller, which overcomes the influence of input saturation on controller design and control performance. Then, the desired control goal is achieved by the sliding mode control method. Through stability analysis, the proposed controller can achieve the desired control goal. Finally, the effectiveness of the proposed algorithm is verified by simulation results and the experimental platform.

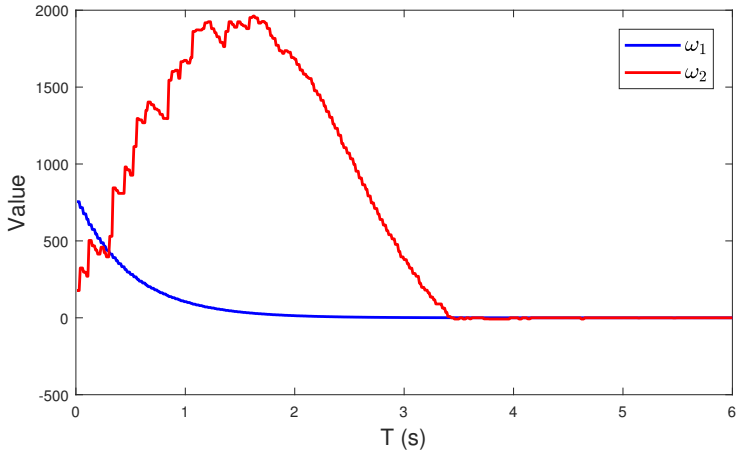

Figure 13. The trajectories of system state of ω_1 and ω_2.

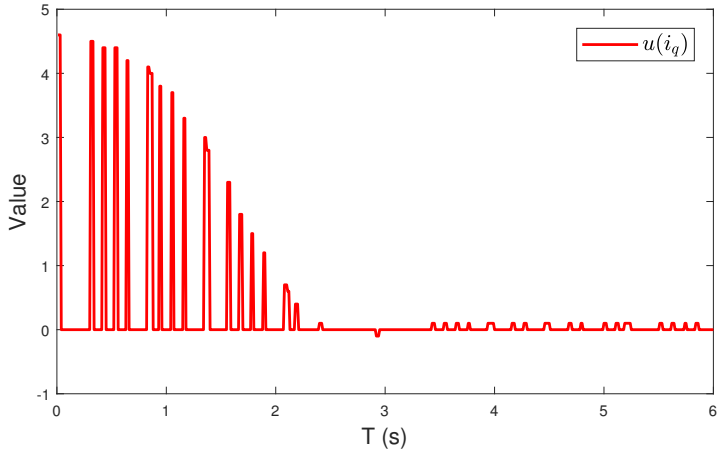

Figure 14. The trajectories of saturated input $u(i_q)$.

Acknowledgments

This work was funded by the National Natural Science Foundation of China under Grant 62173215, Grant 62006192, and Major Basic Research Program of the Natural Science Foundation of Shandong Province in China (ZR2021ZD04).

Conflict of interest

No potential conflict of interest was reported by the author(s).

References

1. D. Yu, J. Long, C. L. P. Chen, Z. Wang, Adaptive swarm control within saturated input based on nonlinear coupling degree, *IEEE Trans. Syst. Man Cybern.: Syst.*, **52** (2022), 4900–4911. https://doi.org/10.1109/TSMC.2021.3102587

2. H. Xu, D. Yu, S. Sui, Y. P. Zhao, C. L. P. Chen, Z. Wang, Nonsingular practical fixed-time adaptive output feedback control of mimo nonlinear systems, *IEEE Trans. Neural Networks Learn. Syst.*, (2022), 1–13. https://doi.org/10.1109/TNNLS.2021.3139230
3. T. Li, X. Sun, G. Lei, Z. Yang, Y. Guo, J. Zhu, Finite-control-set model predictive control of permanent magnet synchronous motor drive systems–an overview, *IEEE-CAA J. Autom. Sin.*, **9** (2022), 2087–2105. https://doi.org/10.1109/JAS.2022.105851
4. T. Zwerger, P. Mercorelli, Using a bivariate polynomial in an ekf for state and inductance estimations in the presence of saturation effects to adaptively control a pmsm, *IEEE Access*, **10** (2022), 111545–111553. https://doi.org/10.1109/ACCESS.2022.3215511
5. Z. Li, T. Li, G. Feng, R. Zhao, Q. Shan, Neural network-based adaptive control for pure-feedback stochastic nonlinear systems with time-varying delays and dead-zone input, *IEEE Trans. Syst. Man Cybern.: Syst.*, **50** (2020), 5317–5329. https://doi.org/10.1109/TSMC.2018.2872421
6. Y. X. Li , G. H. Yang, Observer-based fuzzy adaptive event-triggered control codesign for a class of uncertain nonlinear systems, *IEEE Trans. Fuzzy Syst.*, **26** (2018), 1589–1599. https://doi.org/10.1109/TFUZZ.2017.2735944
7. X. Sun, T. Li, Z. Zhu, G. Lei, Y. Guo, J. Zhu, Speed sensorless model predictive current control based on finite position set for pmshm drives, *IEEE Trans. Transp. Electrif.*, **7** (2021), 2743–2752. https://doi.org/10.1109/TTE.2021.3081436
8. T. Zwerger, P. Mercorelli, Combining a pi controller with an adaptive feedforward control in pmsm, in *2020 21th International Carpathian Control Conference (ICCC)*, (2020), 1–5. https://doi.org/10.1109/ICCC49264.2020.9257288
9. Y. Li, Y. Liu, S. Tong, Observer-based neuro-adaptive optimized control of strict-feedback nonlinear systems with state constraints, *IEEE Trans. Neural Networks Learn. Syst.*, **33** (2022), 3131–3145. https://doi.org/10.1109/TNNLS.2021.3051030
10. X. Xie, T. Wei, X. Li, Hybrid event-triggered approach for quasi-consensus of uncertain multiagent systems with impulsive protocols, *IEEE Trans. Circuits Syst. I-Regul. Pap.*, **69** (2022), 872–883. https://doi.org/10.1109/TCSI.2021.3119065
11. J. Wei, S. Zhang, A. Adaldo, J. Thunberg, X. Hu, K. H. Johansson, Finite-time attitude synchronization with distributed discontinuous protocols, *IEEE Trans. Autom. Control*, **63** (2018), 3608–3615. https://doi.org/10.1109/TAC.2018.2797179
12. Z. Li, L. Chen, Z. Liu, Periodic solution of a chemostat model with variable yield and impulsive state feedback control, *Appl. Math. Model.*, **36** (2012), 1255–1266. https://doi.org/10.1016/j.apm.2011.07.069
13. W. Zhu, D. Wang, L. Liu, G. Feng, Event-based impulsive control of continuous-time dynamic systems and its application to synchronization of memristive neural networks, *IEEE Trans. Neural Networks Learn. Syst.*, **29** (2018), 3599–3609. https://doi.org/10.1109/TNNLS.2017.2731865

14. X. Li, D. Peng, J. Cao, Lyapunov stability for impulsive systems via event-triggered impulsive control, *IEEE Trans. Autom. Control*, **65** (2020), 4908–4913. https://doi.org/10.1109/TAC.2020.2964558
15. X. Li, X. Yang, J. Cao, Event-triggered impulsive control for nonlinear delay systems, *Automatica*, **117** (2020), 108981. https://doi.org/10.1016/j.automatica.2020.108981
16. X. Tan, J. Cao, Intermittent control with double event-driven for leader-following synchronization in complex networks, *Appl. Math. Model.*, **64** (2018), 372–385. https://doi.org/10.1016/j.apm.2018.07.040
17. Z. Wang, C. Mu, S. Hu, C. Chu, X. Li, Modelling the dynamics of regret minimization in large agent populations: a master equation approach, in *Proceedings of the Thirty-First International Joint Conference on Artificial Intelligence (IJCAI-22)* , **23** (2022), 534–540. https://doi.org/10.24963/ijcai.2022/76
18. Y. Yang, Y. He, Non-fragile observer-based robust control for uncertain systems via aperiodically intermittent control, *Inf. Sci.*, **573** (2021), 239–261. https://doi.org/10.1016/j.ins.2021.05.046
19. S. Chen, G. Song, B. C. Zheng, T. Li, Finite-time synchronization of coupled reaction–diffusion neural systems via intermittent control, *Automatica*, **109** (2019), 108564. https://doi.org/10.1016/j.automatica.2019.108564
20. Y. Wu, H. Li, W. Li, Intermittent control strategy for synchronization analysis of time-varying complex dynamical networks, *IEEE Trans. Syst. Man Cybern.: Syst.*, **51** (2021), 3251–3262. https://doi.org/10.1109/TSMC.2019.2920451
21. B. Wang, W. Chen, B. Zhang, Semi-global robust tracking consensus for multi-agent uncertain systems with input saturation via metamorphic low-gain feedback, *Automatica*, **103** (2019), 363–373. https://doi.org/10.1016/j.automatica.2019.02.002
22. V. T. Do , S. G. Lee, Neural integral backstepping hierarchical sliding mode control for a ridable ballbot under uncertainties and input saturation, *IEEE Trans. Syst. Man Cybern.: Syst.*, **51** (2021), 7214–7227. https://doi.org/10.1109/TSMC.2020.2967433
23. X. Yang, B. Zhou, F. Mazenc, J. Lam, Global stabilization of discrete-time linear systems subject to input saturation and time delay, *IEEE Trans. Autom. Control*, **66** (2021), 1345–1352. https://doi.org/10.1109/TAC.2020.2989791
24. Y. Su, Q. Wang, C. Sun, Self-triggered consensus control for linear multi-agent systems with input saturation, *IEEE-CAA J. Autom. Sin.*, **7** (2020), 150–157. https://doi.org/10.1109/JAS.2019.1911837
25. C. Behn, K. Siedler, Adaptive pid-tracking control of muscle-like actuated compliant robotic systems with input constraints, *Appl. Math. Model.*, **67** (2019), 9–21. https://doi.org/10.1016/j.apm.2018.10.012
26. Q. Zhu, Y. Liu, G. Wen, Adaptive neural network control for time-varying state constrained nonlinear stochastic systems with input saturation, *Inf. Sci.*, **527** (2020), 191–209. https://doi.org/10.1016/j.ins.2020.03.055

27. Y. Wu , X. J. Xie, Adaptive fuzzy control for high-order nonlinear time-delay systems with full-state constraints and input saturation, *IEEE Trans. Fuzzy Syst.*, **28** (2020), 1652–1663. https://doi.org/10.1109/TFUZZ.2019.2920808

28. D. Yu, J. Long, C. L. P. Chen, Z. Wang, Bionic tracking-containment control based on smooth transition in communication, *Inf. Sci.*, **587** (2022), 393–407. https://doi.org/10.1016/j.ins.2021.12.060

29. H. Xu, D. Yu, S. Sui, C. L. P. Chen, An event-triggered predefined time decentralized output feedback fuzzy adaptive control method for interconnected systems, *IEEE Trans. Fuzzy Syst.*, (2022), 1–14. https://doi.org/10.1109/TFUZZ.2022.3184834

30. T. Zwerger, P. Mercorelli, Combining smc and mtpa using an ekf to estimate parameters and states of an interior pmsm, in *2019 20th International Carpathian Control Conference (ICCC)*, (2019), 1–6. https://doi.org/10.1109/CarpathianCC.2019.8766063

31. D. Yu, C. L. P. Chen, H. Xu, Fuzzy swarm control based on sliding-mode strategy with self-organized omnidirectional mobile robots system, *IEEE Trans. Syst. Man Cybern.: Syst.*, **52** (2022), 2262–2274. https://doi.org/10.1109/TSMC.2020.3048733

32. D. Shang, X. Li, M. Yin, F. Li, Dynamic modeling and fuzzy compensation sliding mode control for flexible manipulator servo system, *Appl. Math. Model.*, **107** (2022), 530–556. https://doi.org/10.1016/j.apm.2022.02.035

33. N. Zhang, W. Qi, G. Pang, J. Cheng, K. Shi, Observer-based sliding mode control for fuzzy stochastic switching systems with deception attacks, *Appl. Math. Comput.*, **427** (2022), 127153. https://doi.org/10.1016/j.amc.2022.127153

34. W. H. Chen, X. Deng, W. X. Zheng, Sliding-mode control for linear uncertain systems with impulse effects via switching gains, *IEEE Trans. Autom. Control*, **67** (2022), 2044–2051. https://doi.org/10.1109/TAC.2021.3073099

35. L. Y. Hao, J. H. Park, D. Ye, Integral sliding mode fault-tolerant control for uncertain linear systems over networks with signals quantization, *IEEE Trans. Neural Networks Learn. Syst.*, **28** (2017), 2088–2100. https://doi.org/10.1109/TNNLS.2016.2574905

36. A. Vahidi-Moghaddam, A. Rajaei, M. Ayati, Disturbance-observer-based fuzzy terminal sliding mode control for mimo uncertain nonlinear systems, *Appl. Math. Model.*, **70** (2019), 109–127. https://doi.org/10.1016/j.apm.2019.01.010

37. H. Xu, S. Li, D. Yu, C. Chen, T. Li., Adaptive swarm control for high-order self-organized system with unknown heterogeneous nonlinear dynamics and unmeasured states, *Neurocomputing*, **440** (2021), 24–35. https://doi.org/10.1016/j.neucom.2021.01.069

38. B. Jiang, H. R. Karimi, Y. Kao, C. Gao, Takagi–sugeno model based event-triggered fuzzy sliding-mode control of networked control systems with semi-markovian switchings, *IEEE Trans. Fuzzy Syst.*, **28** (2020), 673–683. https://doi.org/10.1109/TFUZZ.2019.2914005

39. G. Wang, J. Kuang, N. Zhao, G. Zhang, D. Xu, Rotor position estimation of pmsm in low-speed region and standstill using zero-voltage vector injection, *IEEE Trans. Power Electron.*, **33** (2018), 7948–7958. https://doi.org/10.1109/TPEL.2017.2767294

40. A. Kolli, O. Béthoux, A. D. Bernardinis, E. Labouré, G. Coquery, Space-vector pwm control synthesis for an h-bridge drive in electric vehicles, *IEEE Trans. Veh. Technol.*, **62** (2013), 2441–2452. https://doi.org/10.1109/TVT.2013.2246202

AIMS Press